Ad Hoc Networks 107 (2020) 102241

Contents lists available at ScienceDirect

Ad Hoc Networks

journal homepage: www.elsevier.com/locate/adhoc

Analysis and adaptive optimization of vehicular safety message communications at intersections

Wang Yanbin[a], Wu Zhuofei[b], Zhao Jing[c,d,*], Li Zhijuan[b], Ma Xiaomin[e]

[a] Department of Industrial Engineering, Harbin Institute of Technology, Harbin, China
[b] Department of Computer Science and Technology, Harbin Engineering University, Harbin, China
[c] School of Software Technology, Dalian University of Technology, Dalian, China
[d] Peng Cheng Laboratory, Cyberspace Security Research Center, Shenzhen, China
[e] College of Science and Engineering, Oral Roberts University, USA

ARTICLE INFO

Article history:
Received 19 December 2019
Revised 31 May 2020
Accepted 2 June 2020
Available online 12 June 2020

Keywords:
Adaptive optimization
Broadcast
Intersection
QoS requirement
VANET

ABSTRACT

Safety-related applications in Vehicular Ad-hoc Networks (VANETs) can help to reduce the number of traffic accidents by periodically broadcasting Basic Safety Messages (BSMs). But considering that the density and topology of VANET change frequently, the Quality of Service (QoS) of safety applications with the fixed transmission parameters would not always meet the requirements of safety-related applications. In this paper, we firstly propose an analytical model to evaluate the performance of the BSM broadcast in VANET at the intersections. The effect of the traffic light is also taken into account by introducing the non-homogeneous Poisson process (NHPP) vehicle distribution, which is simulated by microscopic traffic simulator SUMO and validated by Kolmogorov-Smirnov (K-S) test. Secondly, the number of vehicles in the hidden terminal area and the concurrent transmission area need to be computed by complex integral computations for the proposed analytical model for evaluating the QoS of the safety applications, while the vehicle BSMs provide the vehicle location, speed, and transmission parameters, and these BSMs could be measured and collected in a timely manner to integrate into the analytical model to save the complex integral calculations. Based on the cross-validation QoS metrics between the NS2 (Network Simulator-ns-2) simulation and the analytical model, we employ the vehicle entity of the NS2 simulation model to represent the actual vehicle BSMs, to obtain the number of vehicles in the hidden terminal area and the concurrent transmission area. Finally, to maximize the transmission capacity and minimize the delay under the constraint of maintaining a high application-level QoS of safety applications, a multi-objective optimization scheme with Bare Bones Particle Swarm Optimization (BBPSO) is proposed to dynamically adjust multi transmission parameters. The accuracy of the proposed analytical model is validated by the NS2 simulation. The experimental results also show that the optimized ones could get better results compared with the real test-bed used transmission parameters. Furthermore, the comparisons with slotted-p(or 1)-persistent protocol and CSMA/CA with retransmission strategy show that the proposed solution could make VANET work with better performance at various vehicle densities.

1. Introduction

Vehicular Dedicated Short Range Communication (DSRC) system has been proposed to facilitate VANETs [1,2], exchanging safety-related messages among vehicles to prevent potential traffic accidents. According to the US Department of Transportation (DOT), vehicle-to-vehicle (V2V) communication based on DSRC can address 79% of all crashes in the United States involving unimpaired drivers, which could save thousands of lives and billions of dollars [3]. Two classes of safety-related messages in VANETs have been designed to support various safety-related applications: BSMs in the US or cooperative awareness messages (CAMs) in Europe, and event-driven safety messages (ESMs) in the US or decentralized environmental messages (DENMs) in Europe. Vehicles periodically generate and transmit BSMs carrying the current state information of vehicles, such as position, velocity, direction, and so on. ESMs are generated when an abnormal or emergency event occurs, which is subject to the Poisson process.

Through BSMs, some safety-related applications could be enabled in VANETs, e.g., Cooperative Collision Warning (CCW) [4], Slow Vehicle Indication (SVI) [5], and Rear-end Chain Collision

* Corresponding author.
E-mail addresses: zhaoj9988@dlut.edu.cn (Z. Jing), xma@oru.edu (M. Xiaomin).

https://doi.org/10.1016/j.adhoc.2020.102241
1570-8705/

Table 1
Analytical and simulation models on evaluating broadcast performance.

Model	Scenario	Protocol	V.D.[1]	H.T.[2]	C.C.[3]	F.C.[4]	R.L. [5]	Op.[6]
Hasson 2011 [25]	1-D highway	DCF	HPP	✓	-	-	MAC	retransmission
Yao 2013 [31]	1-D highway	EDCA	HPP	✓	-	-	MAC	-
Ma 2013 [32]	Intersection	DCF	HPP	✓	✓	✓	MAC	-
Ni 2015 [33]	1-D highway	DCF	Log-normal	✓	-	✓	MAC	-
Ma 2016 [34]	Intersection	DCF	NHPP	✓	✓	✓	MAC	-
Nguyen 2016 [35]	1-D highway	TDMA CSMA	HPP	✓	✓	✓	MAC	broadcast frame
Ma 2017 [36]	1-D highway	DCF	HPP	✓	-	✓	MAC	-
Luong 2017 [37]	1-D highway	DCF EDCA	U.[7]	✓	✓	-	MAC	λ
Patel 2017 [38]	1-D highway	EDCA	random	✓	✓	✓	MAC	transmit power
Kühlmorgen 2017 [16]	Intersection	DCF	SUMO-based	✓	✓	✓	APP	joint decoding
Haouari 2018 [17]	1-D highway	DCF	U.	✓	✓	✓	APP	density-aware congestion control
Carpenter 2018 [15]	Urban and Highway	DCF	random	✓	✓	✓	APP	-
Noor 2018 [39]	Intersection	DCF	U.	✓	✓	✓	MAC	-
Kimura 2019 [40]	Intersection	ALOHA	HPP	✓	✓	✓	MAC	λ
Zhao 2019 [13]	1-D highway	DCF	HPP	✓	✓	✓	APP	λ, *W*, *Rd*
Li 2020 [14]	1-D highway	DCF	HPP	✓	✓	✓	APP	λ
Zhao 2020 [41]	*d*-D	DCF	HPP	✓	-	✓	MAC	λ, *W*, *Rd*
proposed model	Intersection	DCF	NHPP	✓	✓	✓	APP	λ, *W*, *Rd*

1. Vehicle Distribution; 2. Hidden Terminal; 3. Concurrent Collisions; 4. Fading Channel; 5. Reliability Level; 6. Optimization; 7. Uniform distribution

Warning (RCW) [6], etc. Since these applications on the road are about life and death, it is very critical for VANETs to support all safety applications with required reliability and performance under all possible vehicular environments and traffic loads. While BSMs and ESMs could get similar performance and reliability when they have the same average message generation intervals [7], the research method and conclusion based on BSMs in this paper can be further extended to ESMs.

VANETs communication could not guarantee a successful broadcast because of the imperfect channel and collision problem. Considering the hidden terminal problem, concurrent transmission and channel fading, various approaches have been deployed to investigate the reliability of VANETs (see Table 1) and formed some commonly used MAC-level QoS metrics, such as Packet Reception Probability (*PRP*), Packet Delivery Ratio (*PDR*) [8], and so on. However, the MAC-level QoS metrics may not be suitable for evaluating the safety-related applications, since different safety-related applications often have their own enabling areas and stringent QoS requirements [9]. To handle this, some general application-level (APP-level) metrics, such as awareness probability in the region of interest (*ROI*) [10] and APP-level delay [11], were developed to promote a rich VANETs evaluation system [12–14] that is closer to the users and facilitate designing and testing new performance improvement solutions [15–17]. The transmission capacity [18,19] is another critical VANETs metric which could reflect the capability that the DSRC communication system could provide to the users [20]. A better transmission capacity could support more vehicles and a higher awareness update ratio. Currently the combination of the transmission capacity and the APP-level reliability has not been well studied in various VANETs scenario, including the signalized intersection, where almost half of all accidents occur each year [21].

In this paper, we propose an analytical and optimization framework for VANETs at a signalized rural intersections, aiming at meeting the QoS requirements of safety-related applications and maximizing transmission capacity and lower the application delay. There are mainly three challenges overcoming in order to apply our analytical and optimization framework for VANET to the actual scene. The first challenge here for building the model is to make the vehicle distribution close to the actual vehicle intersection scene. The Poisson point process of the vehicle locations is always used in the research on the highway scenario who is the most studied (see Table 1). However, it may not a suitable assumption at a traffic lights controlled intersection since the density of vehicles in different sections of the road may vary with the phases of the traffic lights. So we adopted the NHPP assumption of vehicle locations in the proposed analytical model. The intersection vehicle distribution is furthermore simulated by the microscopic traffic simulator SUMO [22] and the theoretical NHPP assumption has been verified to be reasonable via the K-S test.

The second challenge is to minimize the execution time with the help of real-time vehicle BSMs collection. In the analytical model, several critical intermediate parameters, which represent the number of vehicles used to evaluate the impact of the hidden terminal problem and the concurrent collisions, are obtained by the time-consuming operation of integrating the density in the piecewise integral region as shown in the Section 3.1 and the Section 3.2. Considering that the number of vehicles can be directly calculated according to the vehicle BSMs in an actual measurement system, hence the vehicle BSMs of simulation model could also be used to inject into the analytical model to replace the complex integral computations due to the cross-validations between the NS2 and the proposed analytical model. We extend the idea to be a combined measurement and analytical (CMA) model given in the Section 3.4, and the characteristics of fast operation as shown in the Section 5.3 pave the way to apply our proposed optimization scheme in the real-world system.

The third challenge we faced is that the fixed transmission parameters may not always meet the requirements of QoS of safety-related applications because the VANETs topology (e.g. vehicle density, vehicle position) could change frequently. We build the optimization problem aiming at maximizing the transmission capacity of VANETs and maintaining the QoS to meet the requirement of safety-related applications by adaptively adjusting the transmission parameters. There are a couple of parameters that could be adjusted, and the number of their combinations would be enormous, so it is feasible to apply a heuristic algorithm to solve the problem. We apply BBPSO [23] algorithm because no parameters need to be predefined, which could introduce less influence of human factor compared with other heuristic-based algorithms when the hyper-parameters are tuning (such as, simulated annealing, ant colony optimization and so on).

Our proposed analytical and optimization framework could be utilized to analyze the QoS of VANET, reduce the execution time by combining measurements with the analytical model, and ensure the QoS at topology changing environment by multi-parameter optimization. The proposed model and optimization method are general and fit for many actual scenes. There are several popular ap-

proaches proposed in the literature to improve the reliability and performance of broadcast, such as retransmission [24–27], slotted-1-persistent, and slotted-p-persistent [28]. We compare these approaches by the Network Simulator NS2 2.35 [29] with the modified wireless model provided by Chen et al. [30]. For each solution, the APP-level reliability metrics and delay are calculated from the trace file. The details of the simulation set up and the results will be presented in Section 5.6. The major contributions of this paper are three-fold:

(1) We propose an analytical model to evaluate the MAC-level and APP-level performance of BSM-based safety-related services at the signalized intersection by considering the impact of the hidden terminal, concurrent collisions, and the fading channel. The effect of the traffic light is considered by giving a more general non-homogeneous Poisson point (NHPP) distribution.
(2) The microscopic traffic simulator SUMO is adopted to mimic the vehicle intersection scene, and the analytical model NHPP assumption is verified via the K-S test accordingly. The BSMs in the communication measurement system could be used to replace the complex integration process for obtaining the QoS metrics, and reduce the optimization time of the analytical model, thus make our analytical optimization model more adaptable to the practical vehicle DSRC system.
(3) To maintain the reliability of safety-related applications in a highly dynamically changed vehicular environment, we propose a multi-objective adaptive optimization scheme based on BBPSO to adjust transmission parameters with the QoS constraint transmission capacity according to the topology of VANETs.

The remainder of this paper is organized as follows. The related works and background knowledge are introduced in Section 2. In Section 3, an analytical model and its implementation in the real scenario are proposed to characterize the MAC-level and APP-level broadcast reliability of IEEE 802.11p based VANETs at intersections with a non-homogeneous Poisson process (NHPP) vehicle distribution. The definition of QoS constraint transmission capacity and the bare bones PSO based multi-objective optimization scheme are given in Section 4. The experiments and the comparison with other protocols or strategies are shown in Section 5 and the paper is concluded in Section 6.

2. Related work and background

Various works have been proposed to investigate the reliability of VANETs. We first review the related works in this section. And the comparisons between them are listed in Table 1 based on the factors of the hidden terminal, concurrent collision, and fading channel. The Scenario, vehicle distribution assumption, the level of the reliability, and the optimization solutions are also mentioned to reveal the details of each work. In the second part, the background of related concepts and methods are introduced, including NHPP, BBPSO, Nakagami model, and so on. And the third part is the overview of our proposed solution.

2.1. Related work

Several works have been proposed to theoretically characterize the reliability of DSRC VANETs safety message broadcast. Three principal factors could affect the performance of VANET, which are hidden terminal, concurrent collision, and fading channel. And they had been studied well separately [25,31] or synthetically [33] in a one-dimensional (1-D) highway scenario. In the intersection scenario, things could be different due to the traffic light controlled flow or the obstructions from buildings. Kimura et al. [40] modeled the vehicles location in queuing or running segments to simulate the traffic signal effect. The broadcast rate was optimized, but the ALOHA protocol was analyzed as a substitute for CSMA, which is feasible in dense networks as mentioned but not in sparse networks. The broadcast performances at the urban intersection with building obstructions were studied in [39,42]. And relaying methods through RSU are applied in both works to improve the performance. But the signal light impact on the vehicle location is not included. Ni et al. [33] proposed an interference-based capacity analysis for 1-D highway VANETs with fading model and Car-following model. But it needs a huge calculation power when the scenario is extended to two-dimensional, because of the multiple integration operations in the model. Ma et al. [32,34] proposed an analytical model for performance analyses of VANETs safety message broadcast at rural intersections and considered the impact of the traffic light. But these work only take the MAC-level metrics into considerations which may not enough to measure the QoS of a safety-related application.

In recent years, a lot of researches [9,43,44] have been made to bring up APP-level evaluation metrics for quantifying safety effectiveness of the safety applications, such as the APP-level latency and APP-level awareness probability which is on top of the MAC-level metrics. At the same time, some analytical work and simulation work based on the awareness probability have been deployed as shown in Table 1. Among them, some researchers [15–17] studied how to improve the awareness probability accurately by considering packet congestion problem, bursty channel condition, and propagation fading and shadowing influential factors. They calculated and compared the awareness probabilities obtained from NS2 simulation [29], NS3 simulation [45], or Matlab simulation. Therefore, the three factors affecting packet reception are considered to have been included to calculate awareness probabilities (see Table 1).

Haouari et al. [17] considered the mitigation of packet congestion problem affecting the awareness probability, and developed the congestion control algorithm using vehicle density information based on the standard protocol, and found that the awareness probability is improved compared with that of standard protocol. Kühlmorgen et al. [16] studied the multi-path propagation and shadowing effects at intersection which make the awareness distance short, and then will lower the APP-level reliability. They developed the cooperative relaying with joint decoding technique to improve the awareness distance to enhance the APP-level reliability. Carpenter et al. [15] considered the packet generation interval that does not follow the independent and identically distribution, especially at imminent crash conditions packet generation represent bursty characteristic, and these bursty characteristic definitely affect the current channel model to evaluate the APP-level reliability. They built the channel model considering the packet generation algorithm, and found the evaluation accuracy of APP-level reliability improved compared with real-measurements.

Some theoretical analytical models [13,14] of awareness probability were also proposed by considering the impact of hidden terminal, fading channel, and the concurrent collisions. To make the performance of VANETs meeting the stringent QoS requirements of safety-related applications in the 1-D highway scenario, multiple communication parameters are adaptively adjusted by Zhao et al. [13]. It has been verified that their solution could approximate the transmission capacity and maintain the APP-level reliability with a high level at the same time. Li et al. [14] proposed an adaptive beacon generation rate congestion control protocol to reduce the channel congestion and contention according to the density of vehicles. They also proposed an APP-level reliability assessment scheme to evaluate the reliability of safety-related applications at different densities.

Besides, people also concern about how or to what extent the current DSRC VANETs support a given safety-related application with the corresponding QoS requirements. And the transmission capacity analysis of one-hop VANETs has been attracting much attention, which refers to the attempted transmission intensity per unit area [18,46]. A QoS constraints transmission capacity [36] was defined for the broadcast of safety-related applications in VANETs. It refers to the maximum product of packet generation rate and the number of vehicles within the *ROI*, subject to the constrain on the QoS of safety-related applications. Based on this, Zhao et al. [13] proposed an adaptive optimization scheme to improve the performance of the BSMs broadcast in VANETs. And a reliability evaluation scheme [41] for IEEE 802.11 broadcast in a d-dimensional (d-D) scenario is proposed, in which the QoS constraint transmission capacity was maximized. But these works assumed that the vehicle locations follow HPP, which may not accurate in the signalized intersection.

Due to the vehicle density and speed are both dynamically changed, lots of works are trying to improve the QoS of VANETs by adapting Network-layer or MAC-layer parameters. For example, tunning the beaconing frequency [37] according to the VANETs traffic behavior, adjusting the broadcast frame length efficiently to support broadcast services on the control channel [35], adapting transmission power scheme based on transmission range and vehicle density to improve the Average Connected Coverage of VANETs [38], and so on. But these works only adjust one of the transmission parameters, and not include the APP-level QoS of safety-related applications and VANETs capacity at the same time, so they might not utilize most of the channel capacity of the VANETs. With that in mind, an optimization scheme [13] is proposed to adjust several transmission parameters dynamically to maximize the transmission capacity under the constraint of awareness probability. But this work neglects the delay requirement, which is one of the important requirements of the safety-related applications. While in this paper, both of the transmission capacity and the APP-level delay are considered as the optimization goals and multi-parameters are optimized at the same time.

2.2. Background

2.2.1. A general NHPP

At the intersection, the number of vehicles varies between different segments, and they are more likely to locate in a specific segment. This behavior can be captured by using an NHPP [47], i.e., the densities of vehicles are the function of distance from the intersection instead of constant in HPP. Let $N(x)$, $x \geq 0$ be a counting process representing the cumulative number of vehicles by a distance x from the intersection. Let $\beta(x)$ denote the density of vehicles in each segment, Then, the probability of finding i vehicles in a space range $(d, d+l)$ as follows:

$$P[N(x)=i,(d,d+l)]=\frac{(\int_d^{d+l}\beta(x)\mathrm{d}x)^i e^{-\int_d^{d+l}\beta(x)\mathrm{d}x}}{i!} \tag{1}$$

2.2.2. Nakagami fading model

Channel fading and shadowing in wireless communications can cause significant loss and degradation of safety message broadcast. The *Nakagami* distribution is believed to fit the empirical amplitude envelope of the DSRC channel [48]. The probability density function (PDF) of signal amplitude of Y could be expressed as:

$$f_Y(y)=\frac{2m^m y^{2m-1}}{\Gamma(m)\omega^m}e^{my^2/\omega} \tag{2}$$

where $\Gamma(m)$ is the standard Gamma function, m and ω refer fading parameter and average received power respectively. And the PDF of the signal power $Z=Y^2$ is:

$$f_Z(z)=\frac{m^m}{\Gamma(m)\omega^m}z^{m-1}e^{-mz/\omega} \tag{3}$$

2.2.3. Bare bones particle swarm optimization

Heuristic-based optimization methods are popular [49] in VANETs related research, in which the complex real-world problems are involved. In heuristic algorithms, the exploitation and exploration are the two main parts, and the implementations and the weights of these two strategies vary with different algorithms. Among them, the Particle Swarm Optimization (PSO) [50] has a simpler and clearer formula to identify the exploitation and exploration parts.

The PSO imitates the movement of the bird flock. All of the birds would move towards the one who has the closest distance to the food. That means the algorithm searches the solution space according to the current optimal solution iteratively to approximate the global optimal solution to the problem. In the optimization process, each bird stands for a solution to the problem, and the best result is the food.

Comparing with the canonical PSO, the BBPSO [23] is an improved version of PSO with a simpler formula and faster speed, and it has no hyper-parameter should be predefined by people, which could reduce the impact of subjective factors. Because of the advantages mentioned above, the BBPSO is selected as the optimization method in this paper. The iteration function of the BBPSO can be presented as follows:

$$\begin{aligned}\boldsymbol{X}_i^{(k+1)} &= N(\mu_i,\sigma_i^2)\\ \mu_i &= (\boldsymbol{X}_{i,pb}^{(k)}+\boldsymbol{X}_{gb}^{(k)})/2\\ \sigma_i &= |\boldsymbol{X}_{i,pb}^{(k)}-\boldsymbol{X}_{gb}^{(k)}|\end{aligned} \tag{4}$$

where N designates a Gaussian distribution, the position of the i-th particle in the k-th iteration is represented as $\boldsymbol{X}_i^{(k)}=(X_{i,1}^{(k)},X_{i,2}^{(k)},\ldots,X_{i,n}^{(k)})$. n is the number of parameters to be adjusted. And the $\boldsymbol{X}_{i,pb}^{(k)}$ is the best historical location of the i-th particle and the $\boldsymbol{X}_{gb}^{(k)}$ is the best historical global solution. The Eq. (4) shows that the location of the i-th bird in the $(k+1)$-th iteration could be derived from a Gaussian distribution. While the mean and variance are related to the bird flock status in the k-th iteration.

2.2.4. Kolmogorov-Smirnov test

The K-S test is a nonparametric test in statistics that can be used to compare a sample observed from a distribution with a reference probability distribution. Under the null hypothesis, the two distributions are identical. The K–S statistic quantifies a distance between the empirical distribution function $G(x)$ of the sample and the cumulative distribution function $F(x)$ of the reference distribution, as expressed in Eq. (5).

$$D_N=\max_{1\leq i\leq N}(F(Y_i)-\frac{i-1}{N},\frac{i}{N}-F(Y_i)) \tag{5}$$

where the samples are reordered from small to large and Y_i is the i-th sample, N is the total number of the samples. Then the null hypothesis is accepted if

$$\sqrt{N}D_N \leq K_\alpha \tag{6}$$

where α refers to the significance level, K_α is the critical value which could be found in a lookup table given in [51].

2.3. Overview of our solution

The framework of the analysis and optimization process is shown in Fig. 1. This figure combines the analytical model, measurements, and the optimization scheme. On the one hand, the analytical model proposed takes the communication parameters used

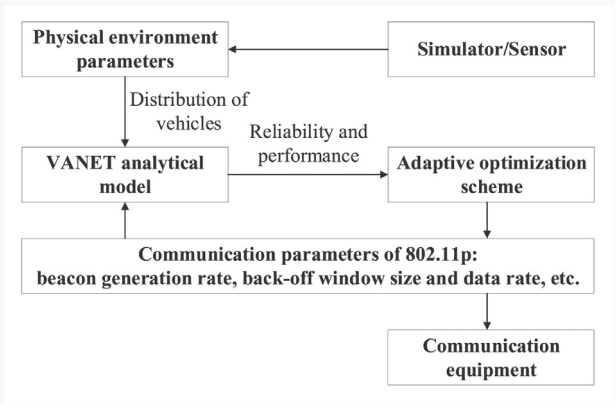

Fig. 1. Framework of the analysis and optimization process.

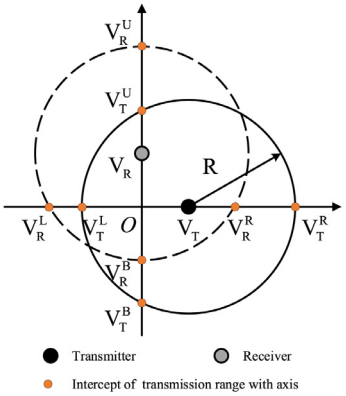

Fig. 2. Abstraction of an intersection.

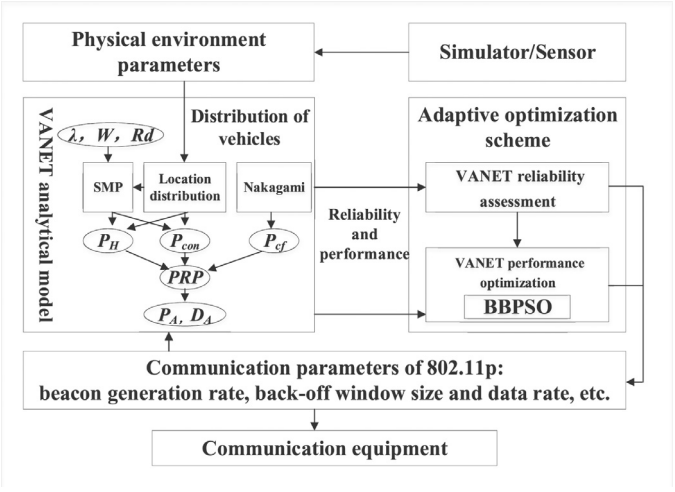

Fig. 3. Detailed framework of the proposed solution.

by the vehicle nodes and the locations of the vehicles as input and then outputs the MAC-level or APP-level reliability metrics. These communication parameters include beacon generation rate λ, back-off window size W, data rate R_d, and so on. The locations of the vehicles could be derived from a specific distribution or collected from the sensors in the real world or a simulator. On the other hand, based on the evaluation QoS, the adaptive optimization scheme would adjust the communication parameters to keep the QoS meeting the requirements of safety-related applications, and then obtain the optimized combination of parameters. The optimized combination of parameters would be deployed in the communication equipment of the actual system.

3. Analytical model of vanets at intersections

In this section, we thoroughly describe the proposed analytical model for deriving the APP-level reliability and performance metrics. We further explore applying the model to actual systems by combining the measurements from the BSMs of the vehicles with the analytical model. Our research and exploration are beneficial to optimize the actual communication system of VANETs due to the following two advantages. On the one hand, the performance and reliability of VANETs in a given scenario can be accurately evaluated by the model because that the NHPP assumption of vehicles has been verified to be reasonable via the K-S test, and the evaluation accuracy will be represented in the Section 5.3. On the other hand, it is easy to deploy our analytical model in the actual system because we give the combined measurements and analytical (CMA) model which integrates the BSMs into the analytical model. Moreover, by using the BSMs information, some complicated integration processes in the analytical model could be replaced by just calculating the number of vehicles in the hidden terminal area and concurrent transmission area from the measurements, and thus the CMA could reduce the execution time to obtain the QoS metrics. For the convenience of analysis, seven assumptions are made for our analytical model as follows.

(1) The model is based on an isolated rural intersection broadcast VANET scenario where the width of the road and the obstructions from buildings are neglected. As abstracted in Fig. 2, the origin is set at the road intersection and the transmitting vehicle V_T is located at coordinate $(x_T, 0)$, and one of the receivers V_R at coordinate (x_R, y_R);
(2) Due to the influence of the traffic light, the vehicles are distributed according to a Non-Homogeneous Poisson Process (NHPP), which is validated in Section 5. $\beta(x)$ and $\beta'(x)$ are denoted as the immediate density of vehicles at a road spot with distance x from the center of the intersection (say, origin (0,0)) in x-axis and y-axis, respectively;
(3) All vehicles in the VANET are equipped with DSRC wireless communication equipment, and have identical transmission range, receiving range, and carrier sensing range, which is denoted as R;
(4) Each vehicle generates packets following the Poisson point process with the rate λ, and the queue length of packets at each vehicle is infinite;
(5) Actual measurements indicated that compared to other models, the *Nakagami* distribution fits the amplitude envelope of signal transmitting on DSRC channel better to VANET [52], so *Nakagami* fading model is assumed for analyzing the impact of channel fading;
(6) Impact of vehicle mobility on the reliability is neglected because the impact of node mobility could be neglected with one-hop broadcast and high data transmission rates [53];
(7) The channel condition sensed by each vehicle is identical.

In this Section and the next, a VANETs analytical model and an adaptive optimization scheme are proposed respectively to dynamically find the suitable communication parameters under the APP-level QoS constrains. A detailed framework of our solution is depicted as Fig. 3. The input of the analytical model consists of the communication parameters (e.g. λ, W and Rd) and the locations of the vehicles, which could be derived from a specific distribution or the sensor in the real world. The probability that a broadcast packet (message) is successfully delivered from the transmitter V_T to the receiver V_R is called packet reception probability (*PRP*). And

Table 2
Summary of symbols.

Sym	Descriptions	Sym	Descriptions
V_T	packet transmitter	V_R	packet receiver
d	m, distance between V_T and V_R	R	m, transmission range
λ	Hz, beacon generation rate	W	contention window size
R_d	Mbps, data rate	β	vehicles/km, density of vehicle
β_{av}	vehicles/km, average density of vehicle	π_{XMT}	steady-state probability that the tagged vehicle is transmitting
π_0	the steady-state probability of a vehicle's back-off timer counts down to zero	q_b	the probability that the channel is busy during *DIFS* time of a tagged vehicle
p_b	the probability that the channel is busy during a back-off time slot of a tagged vehicle	$\overline{n}_\Sigma$	the average number of nodes transmitting in the concurrent slot in the area $[-(R-x), R]$
T	μs, back-off timer suspend time	TR_y	reception threshold
m	param of *Nakagami* distribution	ω	average power received at V_R
P_A	awareness probability	D_A	APP-level delay
T_a	application tolerance window	N_{ROI}	the num of nodes in the ROI
ξ	threshold of P_A	n	packets/sec required by App
n_f	first n_f packets are successfully delivered to the receiver	T_{P_A}	time complexity to compute P_A
T_{D_A}	time complexity to compute D_A	n_p	particle num in PSO
$\boldsymbol{X}_{i,pb}$	the best solution of i-th particle	$\boldsymbol{X}_{gb}$	the best global solution of PSO

three factors need to be considered, which are the impact of the hidden terminal problem (P_H), concurrent transmission collisions (P_{con}), and channel fading with path loss (P_{cf}). The *PRP* can be expressed as

$$PRP = P_H \cdot P_{con} \cdot P_{cf} \tag{7}$$

This paper uses the same semi-Markov processes (SMP) model adopted in [11] for the tagged vehicle to capture the IEEE 802.11p based broadcast channel contention (access). Through solving the SMP model, the following parameters can be derived: (1) π_0: the steady-state probability that the back-off timer of the tagged vehicle counts down to zero; (2) π_{XMT}: the steady-state probability that the tagged vehicle is transmitting; (3) q_b: the probability that the channel is sensed busy for *DIFS* time by a tagged vehicle, where *DIFS* is IEEE 802.11 DCF (distributed coordination function) Interframe Space duration; (4) p_b: the probability that a tagged vehicle senses channel in a busy state during one back-off time slot.

Then the P_H and P_{con} could be derived with these parameters, while the P_{cf} could be calculated from the *Nakagami* model as shown in Fig. 3. Then the APP-level awareness probability P_A and delay D_A could be output to the adaptive optimization scheme. The VANETs reliability assessment and the VANETs performance optimization are two main steps of the adaptive optimization scheme, which could eventually output the suitable communication parameters. This part would be explained in detail in Section 4. To make this paper more readable, the symbols are summarized in Table 2.

3.1. Impact of hidden terminals

According to the CSMA protocol, the time to suspend a back-off timer when a node with packets detects an ongoing transmission can be expressed as:

$$T = (L_H + E[L_p])/R_d + DIFS + \delta \tag{8}$$

where L_H and $E[L_p]$ are the length of the packet header and the average packet length, respectively. R_d represents the system transmission data rate and δ is the propagation delay. Then, the time to transmit a packet is $T - DIFS$. And the probability that a broadcast packet (message) transmission from V_T to V_R is free from the hidden vehicles' transmissions is [7]:

$$P_H(V_T, V_R) = \exp(-2(T - DIFS)\pi^{(1)}_{XMT}\Delta_h/T) \tag{9}$$

where $\pi^{(1)}_{XMT}$ is the steady-state probability that a vehicle in the hidden terminal area is transmitting, which can be obtained in [32] assuming all hidden vehicles are uniformly distributed on a 1-D road, because when the transmitter is close to the intersection, the hidden terminal will be away from the intersection and the effect of traffic light on density can be ignored. Δ_h is the average number of vehicles in the potential hidden terminal area of the tagged vehicle V_T on all lanes at the intersection.

Denoting $\beta(x)$ and $\beta'(y)$ as immediate vehicle densities at the intersection on x-axis and y-axis, respectively, Δ_h can be evaluated considering uneven densities of vehicles in the hidden terminal area as a function of vehicles' location, which is expressed as:

$$\Delta_h = \int_{\min(V_T^L, V_R^L)}^{V_T^L} \beta(x)\mathrm{d}x + \int_{V_T^R}^{\max(V_T^R, V_R^R)} \beta(x)\mathrm{d}x + \int_{V_T^U}^{\max(V_T^U, V_R^U)} \beta'(y)\mathrm{d}y + \int_{\min(V_T^B, V_R^B)}^{V_T^B} \beta'(y)\mathrm{d}y \tag{10}$$

where V^L, V^R, V^U, and V^B represent the four intercepts of a vehicle's transmission range with x-axis and y-axis, which means Left, Right, Upper and Below respectively, as shown in Fig. 2.

3.2. Impact of concurrent collisions

Other than the collisions due to the hidden terminal problem, transmissions in the same slot from vehicles within the interference range of the tagged vehicle, which cannot be detected by CSMA protocol, may also cause packet (message) collisions. The probability that no vehicles transmit on the same slot within the interference range of V_R or the probability that there is no concurrent collision with the transmission from V_T is derived as [32]:

$$P_{con}(V_T, V_R) = q_b \exp(-\overline{n}_\Sigma) + 1 - q_b \tag{11}$$

where $\overline{n}_\Sigma$ is the average number of vehicles who transmit concurrently within the area

$$S = D(V_T, R) \bigcap D(V_R, R) \tag{12}$$

where $D(s, l)$ denotes the disk area with radius l centered at s.

For an interference vehicle V_I in the area S, the probability that it starts transmitting during the slot is

$$\pi_0^{(2)} \cdot P'_H(V_I, V_R) \tag{13}$$

where $\pi_0^{(2)}$ is the probability of vehicle V_I intends to transmit, and $P'_H(V_I, V_R)$ represents the probability of all vehicles in area S_I^c are not in transmitting state,

$$S_I^c = D(V_I, R) \cap [D(V_T, R) \cup D(V_R, R)]'$$

where $D(V_T, R)'$ represents the complementary area of $D(V_T, R)$, $\pi_0^{(2)}$ can be calculated via locating the tagged vehicle at the center of the intersection with the assumption 7), $P'_H(V_I, V_R)$ can be derived in Eq. (14)

$$P'_H(V_I, V_R) = \sum_{i=0}^{\infty}(1 - P_{XMT}^{(1)})^i \frac{N_I^i}{i!} e^{-N_I} = e^{-N_I P_{XMT}^{(1)}} \tag{14}$$

where N_I is the expected number of vehicles in the area S_I^c, which is,

$$N_I = \int_{V_I^L}^{\max(V_I^L, \min(V_T^L, V_R^L))} \beta(x)\mathrm{d}x + \int_{\min(V_I^R, \max(V_T^R, V_R^R))}^{V_I^R} \beta(x)\mathrm{d}x + \int_{V_I^B}^{\max(V_I^B, \min(V_T^B, V_R^B))} \beta'(y)\mathrm{d}y + \int_{\min(V_I^U, \max(V_T^U, V_R^U))}^{V_I^U} \beta'(y)\mathrm{d}y \tag{15}$$

Then $\overline{n}_\Sigma$ can be derived as,

$$\overline{n}_\Sigma = \int_{\max(V_T^L, V_R^L)}^{\min(V_T^R, V_R^R)} \beta(x)\pi_0^{(2)} P'_H(V_I, V_R)\mathrm{d}x + \int_{\max(V_T^B, V_R^B)}^{\min(V_T^U, V_R^U)} \beta'(y)\pi_0^{(2)} P'_H(V_I, V_R)\mathrm{d}y \tag{16}$$

3.3. Impact of fading with path loss

Channel fading and shadowing in wireless communications can cause significant loss and degradation of safety message broadcast. In this paper, the *Nakagami* distribution is used to characterize the fading with path loss as depicted in Eq. (2) and Eq. (3). Then the probability of successfully delivering a message (packet) between two vehicles with distance d can be expressed as [54]

$$P_{cf}(d) = 1 - \frac{m^m}{\Gamma(m)} \int_0^{(d/R)^\gamma} z^{m-1} e^{-mz}\mathrm{d}z \tag{17}$$

where $d = \sqrt{(x_T - x_R)^2 + y_R^2}$, γ is the path loss exponent, which is usually empirically determined by field measurements [55].

3.4. Combined measurement and analytical (CMA) model

In the proposed analytical model, several critical intermediate parameters need to be calculated, such as π_0, P_b, and the number of vehicles related parameters (as shown in Eq. (10), (15) and (16)). Among these parameters, only the number of vehicles related parameters are derived from a specific distribution assumption through complex integration, and the other parameters could be calculated iteratively as mentioned in the above section. While in the real scenario, the vehicle locations can be obtained from GPS or cells directly, and then be broadcast by BSMs. So, a specific vehicle can measure these number of vehicles related parameters through the BSMs which are sent by its neighbors. Therefore, in the real scenario, the number of vehicle related parameters could be fed into the proposed analytical model directly instead of from the time-consuming integration, and then, we get the CMA model.

Here we make another reasonable assumption that the locations of vehicles around the intersection could be obtained in real-time through VANETs in actual situations because they could be sensed, shared, and predicted timely and in high accuracy [56]. Then, the Eq. (10), (15) and (16) in the CMA can be rewritten as,

$$\begin{aligned} \Delta_h &= |S_T - S_R| \\ N_I &= |S_I - S_T - S_R| \\ \overline{n}_\Sigma &= \sum_I \pi_0^{(2)} P'_H(V_I, V_R) \end{aligned} \tag{18}$$

where S_T, S_R, and S_I represent the sets of vehicles which are within the communication ranges of transmitter, receiver and intruder respectively.

3.5. Reliability metrics of MAC-level and application (APP)-level

3.5.1. Packet Reception Probability (PRP)

Putting the impact of the hidden terminal, packet collisions, and channel fading with path loss together, the *PRP* that a successful packet delivery from the vehicle V_T to the vehicle V_R can be expressed as:

$$PRP(V_T, V_R) = P_H(V_T, V_R) P_{con}(V_T, V_R) P_{cf}(d) \tag{19}$$

3.5.2. Awareness probability (P_A)

It is the probability of successfully delivering at least n packets (messages) from a broadcast vehicle to a receiver, within the application tolerance window T_a. It can be derived with the result of Eq. (19):

$$P_A(n, T_a) = \sum_{k=n}^{\lfloor \lambda T_a \rfloor} \binom{\lfloor \lambda T_a \rfloor}{k} PRP^k (1 - PRP)^{\lfloor \lambda T_a \rfloor - k} \tag{20}$$

3.5.3. APP-level Delay (D_A)

The time interval between the instant that the first broadcast packet generated in the transmitter and the instant that the first n_f packets are successfully delivered to the receiver within a given time interval T_a is defined as APP-level delay D_A. This metric could reflect the updating rate of the information, the shorter of this time, the more accurate state of the transmitter could be captured by the receivers. Denote d as the distance between the transmitting vehicle and the receiving vehicle, the average APP-level delay is formulated as

$$\begin{aligned} E[D_A(d, n_f, T_a)] &= \frac{\sum_{i=0}^{\lfloor \lambda T_a \rfloor - n_f} [(n_f + i - 1)/\lambda + E[D]] P_i}{\sum_{i=0}^{\lfloor \lambda T_a \rfloor - n} P_i} \\ P_i &= \binom{n_f + i - 1}{i} PRP^{n_f}(d)(1 - PRP(d))^i \end{aligned} \tag{21}$$

where P_i represents the probability that the $(n_f + i)$-th packet sent by the transmitter is the n_f-th packet successfully received by the receiver. $E[D]$ is the mean medium service time (because of back-off and packet transmission, etc.) of a beacon message, which can be derived in [11].

4. Transmission capacity and optimization

In this section, we define the optimization issue and give a two-step multi-parameter optimization scheme. We introduce the QoS constraint transmission capacity firstly and then give the algorithm for QoS assessment for the step 1, based on step 1, the VANET performance optimization Algorithm 2 is utilized to do multi-objective optimization at step 2. The purpose of this scheme is to improve the transmission capacity of VANET while keeping its performance meeting the stringent APP-level QoS of the safety-related application such as awareness probability, App-level delay. In a topology changing frequently VANET physical environment of the specific safety-related application (e.g. CCW), the awareness probability and the APP-level delay may not satisfy the requirement of QoS, the optimization scheme can be carried out in the actual system as an effective solution.

4.1. The QoS constraint transmission capacity

ROI is the geographical region covered by the transmitter who participates in a specific application [7,43]. So different safety-related applications would have variant *ROIs*. And the N_{ROI} refers to the number of nodes within the *ROI*, who have installed the same

Table 3
The QoS requirements of typical safety-related applications.

App	d	T_a	n	ξ
CCW	400 m	1 s	1	99.0%
SVI	100 m	1 s	3	99.9%
RCW	50 m	1 s	5	99.9%

application of the transmitter. Based on these notations, the QoS constraint transmission capacity (TC) [46] could be defined as:

$$TC = \max\left(N_{ROI}\lambda\right) \quad \text{subject to} \quad P_A(\lambda, W, R_d) \geq \xi \tag{22}$$

where the packet generation rate λ is one of the optimization communication settings that makes the one-hop surrounding vehicles could meet the QoS requirement of a specific safety-related application. The P_A is the APP-level reliability calculating from the last Section. And the ξ is the QoS requirement of a specific safety-related application [57].

As shown in Table 3, we choose three BSM based safety-related applications with stringent requirements of QoS [58], which are CCW [4], SVI [5], and RCW [6]. This table means that in T_a seconds, at least n packets should be broadcast to the receiver within the radius d of ROI with the probability no less then ξ.

Although the topologies of VANETs change frequently, in a specific time slot, the number of vehicles around the transmitter is more likely to maintain the same, so the N_{ROI} would not change. To approximate the transmission capacity, the λ needs to be set as large as possible. In the meantime, the low-level delay should be maintained to guarantee the APP-level information update rate, thus, the APP-level delay D_A should also be considered. So, the optimization goals and constraints can be formulated as Eq. (23).

$$\begin{aligned} &\min D_A(d, n_f, T_a) \\ &\lambda_{\max} = \arg\max_{\lambda} TC(N_{ROI}, \lambda) \\ &\text{subject to} \quad P_A(\lambda, W, R_d) \geq \xi \end{aligned} \tag{23}$$

4.2. Approximating the transmission capacity

Several parameters could affect the awareness probability P_A together with λ, and each of them has a relatively large range to be adjusted. In this case, the number of combinations of the transmission parameters would be enormous. While in VANETs, it is important that the optimization communication parameters could be calculated timely. As mentioned in Section 2.2.3, the proposed optimization scheme is based on the BBPSO, because it has fast speed, simple formula, and less subjective influence. And there are two main steps in the proposed optimization scheme to adapt the transmission parameters: (1) assessing the system reliability and (2) optimizing the communication settings.

For a transmitter V_T in a specific location, the first step is to assess whether the surroundings could meet the safety-related application requirement ($P_A > \xi$), where ξ represents the threshold of APP-level QoS requirement and P_A can be derived from the Section 3. If not, it means the capacity of VANETs could not support the safety-related application, and then it should take other methods into considerations, for example, borrow the spectrum resources of other channels from the same system or other networks, like LTE network, TV network WiMAX and so on, which is not in the scope of this article.

If the assessing process found at least one set of communication parameters that could meet the APP-level requirement of the specific safety-related application, the optimization process could be started, and the TC can be approximated under the requirement of QoS.

4.2.1. Step 1: VANETs reliability assessment

As shown in Table 3, each safety-related application has its own APP-level QoS requirement, and some of them might be very stringent. So, instead of optimizing the transmission parameters directly, the reliability of VANETs should be assessed first, in case of wasting computing resources when the requirements are too stringent.

A combination of transmission parameters, such as (λ, W, R_d), is a point in the solution space. In the assessing process, several points would be randomly set among this space to find whether there are points that could meet the APP-level QoS requirement. And this process can be iterated for a couple of times. At each time, the awareness probability P_A will be derived from the corresponding point, and the biggest one, P_{Amax}, would be compared with the threshold ξ.

If $P_{Amax} > \xi$, it means that the local environment of the VANET can meet the requirement of the specific safety-related application, and the optimization step could be started. Else, if $P_{Amax} < \xi$ in every iteration, there is a high possibility that the optimization would be useless, and the other measures should be taken. The pseudo-code is presented in Algorithm 1, in which the $\lambda_{\boldsymbol{X}}$, $W_{\boldsymbol{X}}$, $R_{d\boldsymbol{X}}$ present the values of corresponding parameters in the point $\boldsymbol{X}$.

Algorithm 1 VANETs reliability assessment.

Input: $n, T_a, \xi, \beta(x), \beta'(y), V_T, V_R, E[L_p], L_H, \delta, DIFS$.
Output: the evaluation result: True or False.

```
for each iteration do
    Initialize each point X and calculate the awareness probability P_A(X)
    Choose the point with the biggest P_A from all particles as P_Amax
    if P_Amax ≥ ξ then return True end if
    if Iteration times equals the maximum then return False end if
end for
```

Algorithm 2 Multi-objective optimizing process.

Input: $n, T_a, \xi, \beta(x), \beta'(y), V_R, V_T, E[L_p], L_H, \delta, DIFS$.
Output: $\boldsymbol{X}$ with the biggest λ and lowest D_A, where $P_A(\boldsymbol{X}) \geq \xi$.

```
for each particle X do
    X ← rand(λ_X, W_X, R_dX), X_pb ← None
end for
X_gb ← None
for each round of iteration do
    for each particle X do
        Calculate awareness probability P_A(X), APP-level delay D_A(X)
        if X_pb = None and P_A ≥ ξ then X_pb ← X end if
    end for
    for each X in {particles|P_A(X) ≥ ξ} do
        if X_gb = None then X_gb ← X end if
        if λ_X > λ_X_gb then X_gb ← X
        else if λ_X = λ_X_gb and D_A(X) < D_A(X_gb) then X_gb ← X end if
        if λ_X > λ_X_pb then X_pb ← X
        else if λ_X = λ_X_pb and D_A(X) < D_A(X_pb) then X_pb ← X end if
    end for
    update position of each particle X with Eq. (4)
end for
```

Table 4
Parameters of transmission and circumstance.

Params	λ Hz	W	R_d Mbps	$DIFS$μs	σ μs	R m	$E[L_P]$ bytes	L_H bits
Test-bed used (Control group)	10	15	24	64	16	500	200	400
Range	(10,40)	(15,1023)	(3,54)	––	––	––	––	––

4.2.2. Step 2: VANETs performance optimization

If the assessment process returns True, it means that the local VANET environment could meet the APP-level QoS requirement of the application. Then the transmission capacity would be optimized to approximate the maximum utilization of the VANET.

As Eq. (23) described, the transmission capacity is related to the number of vehicles around the transmitter and the beacon generation rate. The latter parameter is the one that can be adjusted, and the BBPSO is used to optimize the *TC*. At each iteration, the largest λ would be found among the particles who meet the requirement of the safety-related application ($P_A > \xi$). The optimization steps are described as follows:

(1) Initialize the transmission parameters of the VANET analytical model;
(2) Randomly set the positions of particles among the solution space with the swarm size n_p;
(3) Derive the awareness probability P_A with the analytical model proposed in Section 3.
(4) Collect the particles who meet the requirement ($P_A > \xi$) as a satisfying set.
(5) Update the $X_{i,pb}$ and X_{gb} according to λ;
(6) Update the position of each particle with Eq. (4);
(7) Repeat step 3 to step 5 until the termination condition is reached;
(8) Output the current global optimal value and end the algorithm.

4.3. The time complexity of the optimization model

The adaptive optimization scheme needs to find suitable transmission parameters in time to fit the dynamically changing environment. So it is necessary to figure out the time complexity of the optimization model.

The analytical model which could evaluate the performance of the BSM broadcast in VANET is the basic part of the adaptive optimization scheme proposed in this paper. There are various analytical models to derive the *PRP* from the transmission parameters of VANET, and the time complexity to calculate the awareness probability would vary. Let the time complexity of this process is represented by T_{P_A}, which is independent of data volume and would vary with different models and their accuracy. The parameters shown in Table 4 are set similar with the ones often used in test-bed [59], and NS2-based simulation [60]. Table 4 shows the controlled parameters for CSMA which are the contention window W, DCF interframe space $DIFS$, and slot time σ. Table 4 also shows the packet header size L_H including the MAC layer header and PHY layer header, the average BSM payload size $E[L_p]$, and application layer packet generation rate λ. We take the parameter value combination in Table 4 as the default control group for the baseline to do the comparisons with the optimized parameter value combinations whose ranges are also indicated as in the Table. The parameter value combination in the control group is from the test-bed which generally denotes the simulation, the emulation, and the actual DSRC system. We mainly focus on the simulation, and the analytical model as test-bed for experiments in the paper. Based on these parameters, the mean execution time of the analytical model over 7 experiments is 19.95 ms, while it is 1.20 ms when the analytical model is combined with the simulation (see Fig. 6).

Let the $n_p \in [10, 100]$ represents the number of particles, $n_{1st} \in [10, 100]$ and $n_{2nd} \in [10, 100]$ stand for the maximum iterations in the first and second step, respectively. Then, for each iteration of step 1, there are two main sub-steps, (1) initializing every particle and calculating the awareness probability P_A from them, and (2) finding the biggest P_A from sub-step (1) and comparing it with the requirement ξ of the specific safety-related application. The time complexities of these two processes are $O((1+T_{P_A})n_p)$ and $O(n_p+1)$, where the T_{P_A} is approximately constant in a specific numerical model. The time complexity of Step 1 can be derived as:

$$(O((1+T_{P_A})n_p)+O(n_p+1))O(n_{1st}) = O(n_p)O(n_{1st}) \tag{24}$$

Step 2 consists of initialization and a BBPSO algorithm. And for each iteration in the BBPSO, there are calculating the awareness probability and APP-level delay of each particle, updating the global and local optimum positions for each particle, and updating their positions. Then, the total time complexity would be:

$$O(n_p)+((T_{P_A}+T_{D_A})O(n_p)+2O(n_p)+O(n_p))O(n_{2nd}) = O(n_p)O(n_{2nd}) \tag{25}$$

where T_{D_A} represents the time complexity of calculating the APP-level delay. As shown in Eq. (21), it relates to the *PRP* and the parameter n_f, which could be determined when given a specific analytical model and a specific safety-related application. So when calculating the time complexity of the optimization model, the T_{D_A} could also be treated as a constant just as the T_{P_A}.

As the above two equations showed, the adaptive optimization scheme only adds the linear time complexity over the original analytical model, so it can meet the requirement of timeliness.

5. Experiments

5.1. Microscopic traffic simulation

The proposed models are applied in a signalized intersection and assumed the vehicle distribution is following the NHPP as shown in Eq. 1. So in this section, we validate this assumption by simulating the traffic at the signalized intersection and processing a K-S test.

The microscopic traffic around an isolated signalized intersection is simulated by SUMO. As shown in Fig. 4, there are four roads connecting to the junction, each road has two directions, 4 lanes in each direction. The yellow triangles stand for the vehicles and the red and green lines represent the signal lights. Every vehicle driving into the scenario at the end of each road. The length of each road is set to 1500 m to mimic the vehicle behavior at the signalized intersections. The intersection does not allow left or right turn and the cycle of the signal light is 60 s (30 s for a green light and 30 s for a red light). The simulation settings are listed in Table 5.

The locations of vehicles are logged in three sections of each road, which are (0, 50) m, (50,100) m, and (100, 500) m away from the intersection respectively. The logs between 540 s and 16500 s with a measurement collection at step of 1 s are analyzed. In every cycle of the signal light there include logs of 60 s, we will analyze the logs from 10 s till 60 s with 5 s step increment. The K-S test and the critical values are used to estimate whether the distributions in each road section following the HPP assumption, so

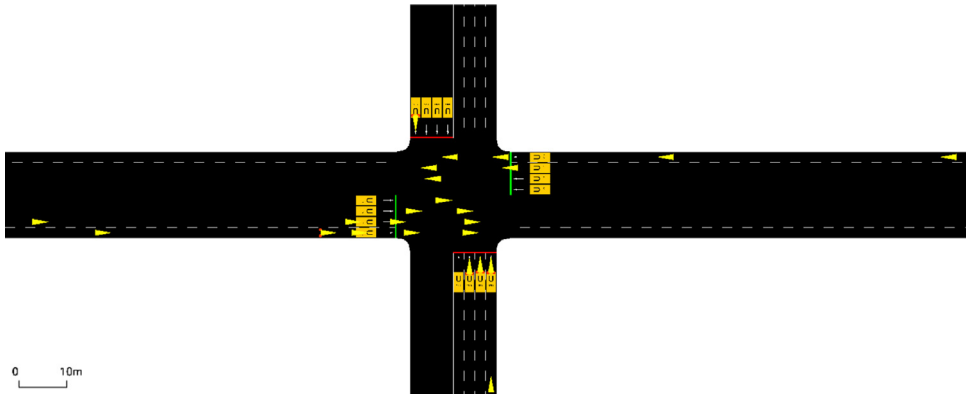

Fig. 4. The microscopic traffic simulation snapshots in the 787^{th} second.

Table 5
Settings of microscopic traffic simulation.

Parameters	Settings	Parameters	Settings
num of roads	4	lanes / road	8
length of roads	1500 m	simulation time	17000 s
driving model	Car-Following-Model	total traffic	5000 cars/road
acceleration	1.25 m/s^2	deceleration	6 m/s^2
cycle of signal	60 s	maximum speed	60 km/h

that the locations of vehicles would follow the NHPP assumption in the road section (0, 500) m, represented as the piecewise (0,50) m, (50,100) m, and (100,500) m. The percentages of the test accept the h_0 hypothesis are shown in Table 6.

The results in Table 6 depict that in most of the time of a signalized intersection, the distribution of the vehicles could be described as a piecewise HPP model or an NHPP model in general, and the second assumption in Section 3 is reasonable.

5.2. The model settings in the experiments

The algorithms are implemented with Python 3.6 on a normal personal laptop. Typical DSRC communication environment and configuration is deployed with communication parameters configured as those in [32]. *Nakagami* channel model is adopted with $\gamma = 2$ and the fading parameter m:

$$\begin{cases} m = 3, & d \le 50\text{m} \\ m = 1.5, & 50 < d \le 150\text{m} \\ m = 1, & d > 150\text{m} \end{cases}$$

where d is communication distance between the transmitter and the receiver. We assume the vehicles at the intersection are distributed with non-homogeneous distribution (piecewise constant) because of the impact of traffic light (β_x for the road with red light; $\beta'(y)$ for the road with green light). The density varies as a function of the distance away from the intersection:

$$\beta(x) = \begin{cases} 3\beta_{av}/2, & x \le 50\text{m} \\ \beta_{av}/2, & 50\text{m} < x \le 100\text{m} \\ \beta_{av}, & x > 100\text{m} \end{cases} \tag{26}$$

$$\beta'(y) = \begin{cases} \beta_{av}/2, & y \le 50\text{m} \\ 3\beta_{av}/2, & 50\text{m} < y \le 100\text{m} \\ \beta_{av}, & y > 100\text{m} \end{cases} \tag{27}$$

where β_{av} (vehicles/km) is a constant average intersection density given a chosen time. The real test-beds used transmission parameters are set as a control group and the parameters to be optimized are also listed, as shown in Table 4.

Meanwhile, the closer the vehicles get to the center of the intersection, the more important the traffic information is, because there are relatively more accidents at the center of the intersection than other parts. Thus the transmitter would locate at (0, 0), the center of the crossroad in the experiment, and the receiver would be set at the edge of the ROI of the corresponding safety-related applications (see Table 3), e.g. 400 m away from the transmitter for CCW, 100 m and 50 m for SVI and RCW respectively.

As for APP-level delay proposed in this paper, it relates to the number of successfully delivered packets n_f. Thus we set it to the same value as the minimal number of received packets n in unit time required by specific safety-related applications.

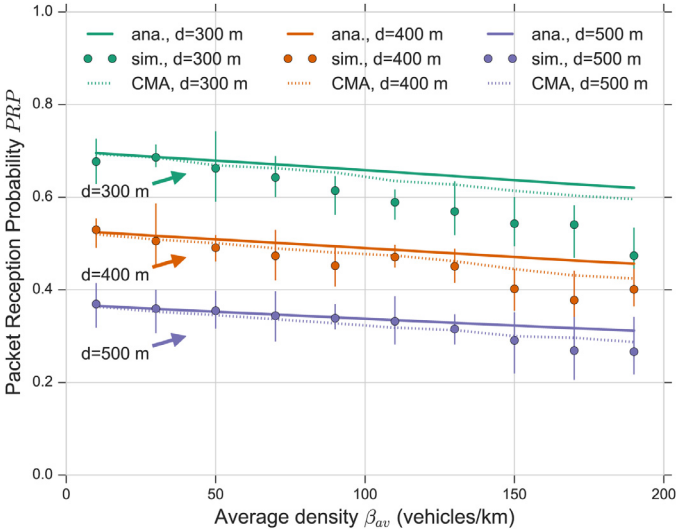

Fig. 5. *PRP*s derived from the analytical model and the NS2 simulation.

5.3. Model cross-validation

In this section, the network simulator NS2 is used to validate or verify the correctness of the proposed analytical model. The parameters and channel model used in the simulation are the same as the analytical model. The parameters are set according to the test-bed used parameters as shown in Table 4. The vehicles are placed at an intersection following the NHPP, and the length of each road is 1000 meters. The transmitter is set at the center of the intersection and the receivers are placed at different positions in x-axis (the road with red light).

Fig. 5 compares the *PRP*s obtained by the analytical model and the NS2 simulation with the receiving distance of 300 m, 400 m, and 500 m, respectively. Each solid or dashed line is made up of the *PRP*s with different densities varying from 10 (vehicles/km) to

Table 6
The ratio of the K-S test accepts the h_0 hypothesis.

second in signal cycle (60 s)	10	15	20	25	40	45	50	55
(0, 50) m	0.996	0.992	0.996	1.000	0.996	0.992	0.996	1.000
(50,100) m	0.958	0.996	0.996	0.996	0.957	0.996	0.996	0.996
(100, 500) m	0.992	0.985	0.910	0.951	0.992	0.985	0.909	0.951

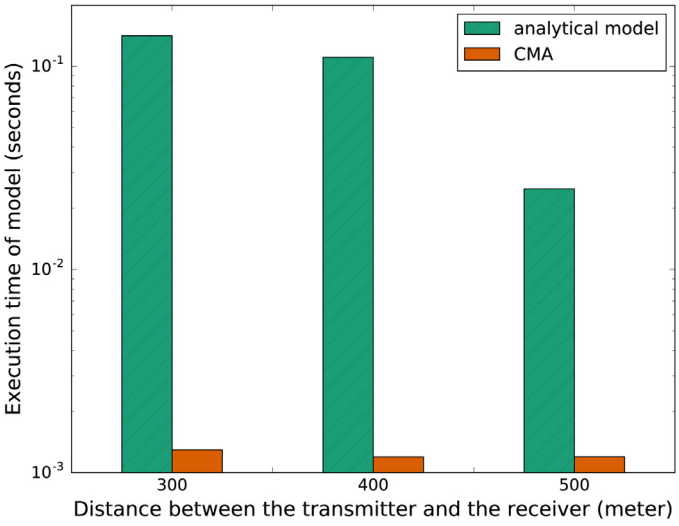

Fig. 6. Execution time of analytical model and the CMA model.

190 (vehicles/km), at the same receiving distance. The obtained *PRP*s from the simulation are an average of 7 independent 20-seconds simulations, and the range of the simulation results are also plotted. It is observed from Fig. 5 that the cross-validations between analytical model and simulation model are very well, so based on the cross-validations, the number of vehicles related parameters derived from the NS2 simulations are used as a substitution of measuring from BSMs, and hence combined the measurements with the analytical model, indicated as CMA model shown in the Fig. 5. The results in Fig. 5 illustrated that the *PRP*s derived by the proposed model and the CMA are very close to the simulation results. This means that the analytical model could reflect the characteristics of the VANET in the signalized intersection. The *PRP*s degrade while the density or the receiving distance increase, this is because the greater the density or the further the distance, the more vehicles will appear in the concurrent collision area or the hidden terminal area, and there will be much interference.

Fig. 5 depicts that at a fixed transmission distance d, the *PRP*s degrade with the increasing vehicle density. This is because when the density increase, there will be more vehicles in the concurrent transmission area and hidden terminal area, then the concurrent transmission probability will rise, which could decrease the *PRP*s. Another phenomenon can be observed in Fig. 5 is that the errors between the simulation and the analytical model increase when the transmission distance d decreases. This phenomenon could be explained as follows. At the real VANET scene, when the target vehicle gets close to the center of the intersection, i.e., the transmission distance d vary from $d = 500$ m to $d = 400$ m to $d = 300$ m, there will be more vehicles participate in competing access channel, then the tagged vehicle will have a lower transmission probability $\pi_0^{(2)}$ (see Eq. (13)), thus the concurrent collision probability becomes large. The simulation model is similar to the actual VANET scene. But to simplify the analytical model, we assume all of the interference vehicles have the same transmission probability $\pi_0^{(2)}$, and this same transmission probability assumption make the target transmitter in the common transmission area have lower concurrent collision probability compared with the simulation model, and hence make the deviations between the simulation model and the analytical model larger with the decreasing distance. It is also explained that we observe that the value of the analytical model is more optimistic than that of the simulation model.

As described in the Section 3.4, Fig. 6 shows the execution time of the analytical model and the CMA with receiving distances, it is seen that the time cost based on CMA could be greatly decreased compared with the analytical model since the complex integration operations in the analytical model are replaced with the real-time measurements of vehicle numbers for the hidden terminal and concurrent transmission area, and also ensure the com-

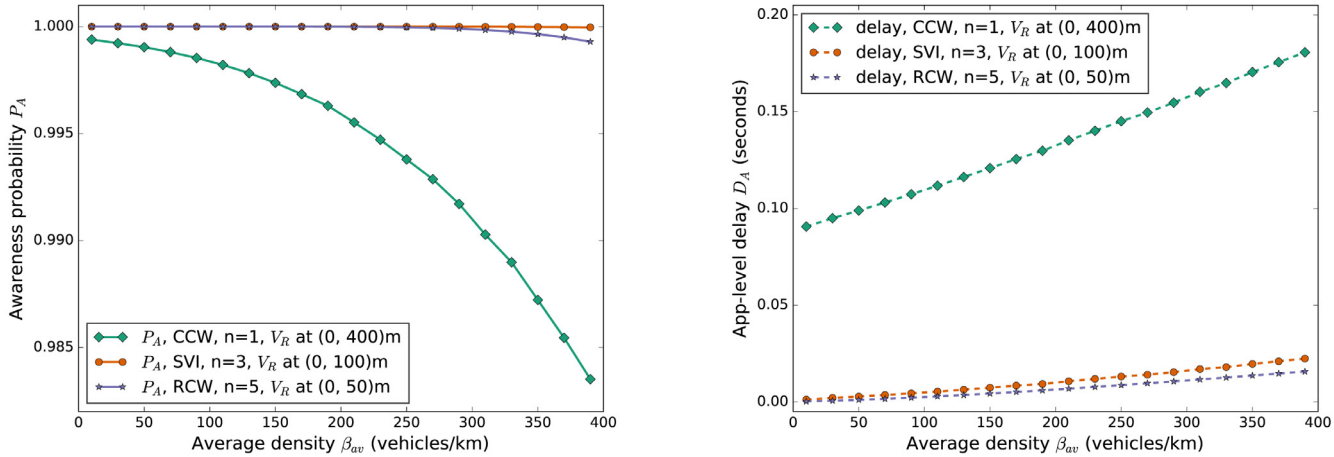

(a) Awareness probability varies with average density (b) APP-level delay varies with average density

Fig. 7. Reliability and performance of the VANET derived from test-bed used parameters with different density of vehicle.

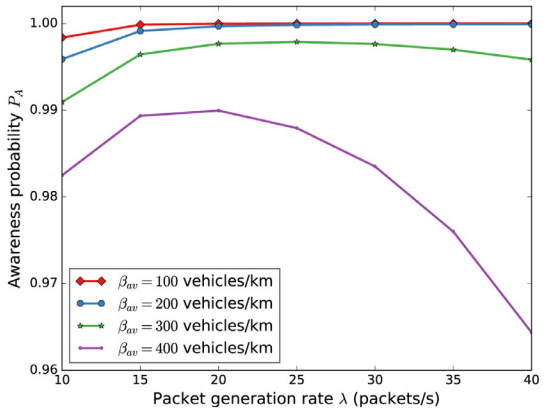

(a) Awareness probability varies with the packet generation rate

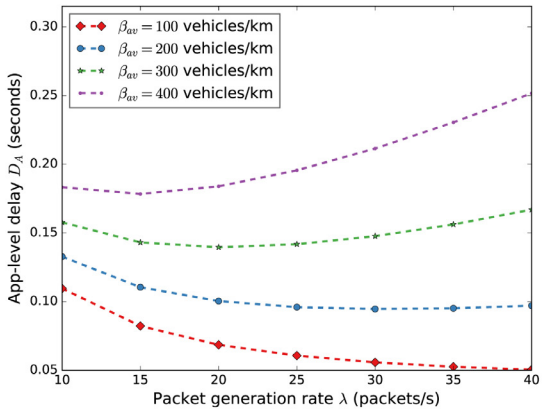

(b) APP-level delay varies with the packet generation rate

Fig. 8. Reliability and performance of the VANET with single parameter Optimization on CCW application.

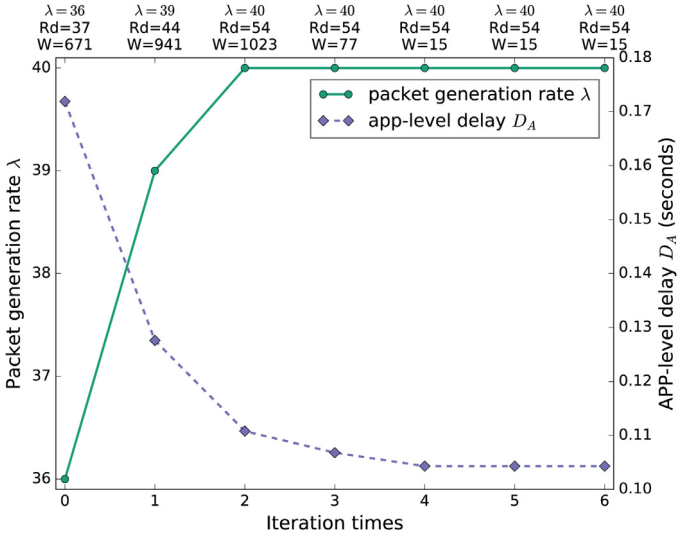

Fig. 9. The log of optimization process.

puting *PRP*s accuracy shown in Fig. 5. Here, the measurements are virtual vehicle locations time series in NS2 simulation along with the simulator execution, and the measurements are collected into the trace-file which are injected into the analytical model to compute the *PRP*s. It is also seen that the execution time of the analytical model declines with the receiving distance, since the larger distance, the less common area *S*, then the fewer integral process to be done (see Eq. (15) and (16)). Although the measurements are collected from the simulation, our analytical model could have strong scalability and adaptability when it was applied in the real system.

5.4. Effectiveness of the fixed parameters

Because of the relatively high speed of the vehicles and frequently changed the topology of the VANET, fixed transmission parameters may not be the best choice to maintain reliability or performance of VANET.

Fig. 7 shows the APP-level reliability (solid lines) and delay (dashed lines) vary with the average density of vehicles applying the test-bed used transmission parameters. Compared with Table 3, the reliability and performance of the VANET may not meet the requirements of some safety-related applications when the density of vehicle increases, e.g. If $\beta_{av} \geq 300$, the P_A of the CCW application will be lower than its requirement ($\xi = 99.0\%$). In this case, an adaptive optimization method is needed to keep high performance by adjusting transmission parameters. Fig. 7 also shows that APP-level delay is different with *CCW*, *SVI*, and *RCW*, it is observed that the APP-level delay increases with the vehicle densities, and it is also seen that the *CCW* has the largest delay compared to the other two.

5.5. Multi-objective single parameter optimization

Taking the safety-related application CCW as an example, the transmitter and receiver are located in the road at (0,0) and (400,0) respectively. With the constraint of $P_A \geq 99.0\%$, the packet generation rate λ could be adjusted to maximize the transmission capacity *TC* and minimize the APP-level delay $E[D_A]$ at the same time.

Fig. 8 shows the effect of packet generation rate λ on the awareness probability P_A (solid lines) and APP-level delay D_A (dashed lines), and the rest transmission parameters are same with the test-beds used. With the increment of the λ, the reliability, and performance improve first and then followed with a long decrease. This is because a higher packet generation rate adds more broadcast transmissions within a unit time, and increases the successful packet delivery probability. But when λ keeps increasing to a certain point, it adds traffic in the MAC-level communication channel and hence message broadcast suffers more severe influence from the concurrent transmissions and hidden terminal transmissions.

On the other side, Fig. 8 also illustrates that joint optimization of multiple parameters is necessary, for example, when $\beta_{av} = 400$ the largest P_A still could not meet the requirement of CCW. And at the most of the situations, larger λ and lower D_A could not be obtained at the same time.

5.6. Multi-objective multi-parameter adaptive optimization

Fig. 9 shows the process of multi-objective multi-parameter adaptive optimization when the average density $\beta_{av} = 400$, and the parameters λ, *W* and R_d are optimized simultaneously. The value of parameters after each iteration are shown at the top of the figure, and with the corresponding parameters, the transmission capacity (which can be represented by λ, see section 4.1) and the APP-level delay could be plotted in green solid line and purple dashed line respectively. After a few iterations, the best transmission parameter set ($\lambda = 40, W = 15, R_d = 54$) can be ob-

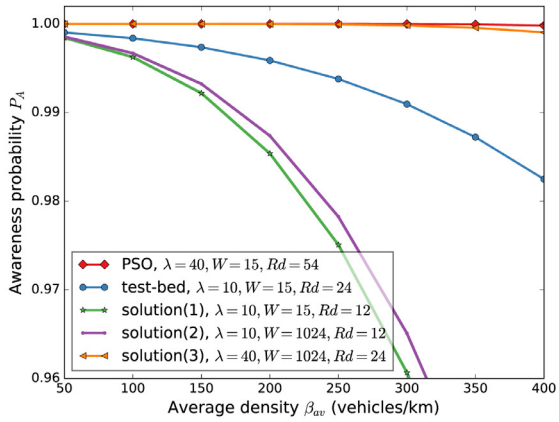

(a) Awareness probabilities derived from different solutions

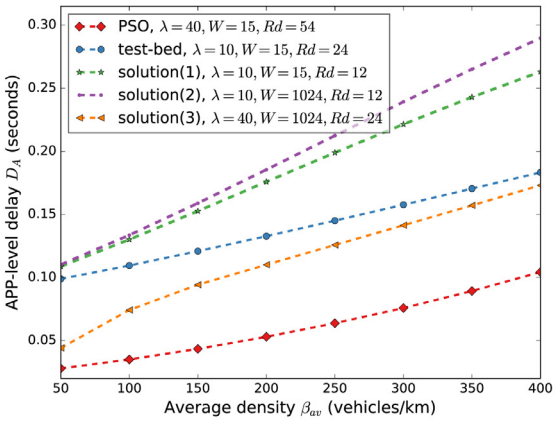

(b) APP-level delay derived from different solutions

Fig. 10. Comparison of P_As and D_As with different communication parameters.

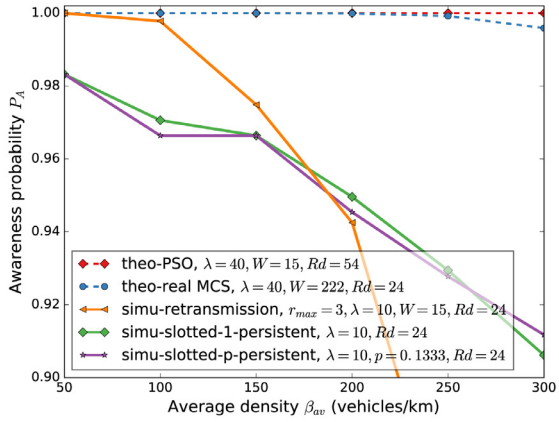

(a) Awareness probabilities derived from different solutions

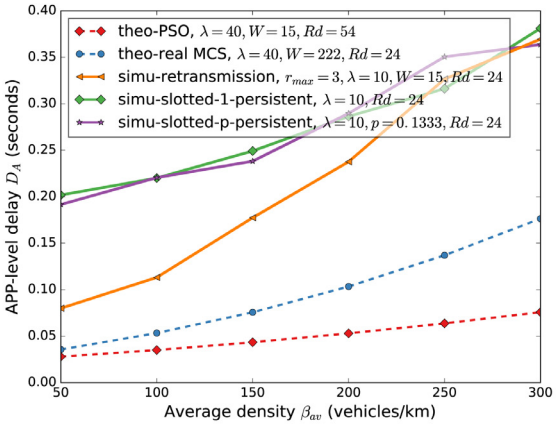

(b) APP-level delay derived from different solutions

Fig. 11. Comparison of P_As and D_As with different communication parameters.

tained for safety-related application CCW under the average density $\beta_{av} = 400$.

The results of different combinations of parameters varying with average density are shown in Fig. 10. The solid lines and dashed lines represent the P_A and D_A respectively, and the red lines are derived from the optimized parameters, the blue lines are calculated from the test-bed used parameters, others apply the parameters randomly combined in [59].

It can be seen the optimized parameters have a big advantage than others, although the solution(3) in the figure can get a similar awareness probability, the optimized parameters still have a significantly lower delay. So, the multi-objective multi-parameter optimization can get a larger λ and a lower D_A at the same time.

Besides, the NS2 simulation results of other MAC protocols are also given in Fig. 11, such as slotted-1-persistent, slotted-p-persistent protocols and retransmission strategy. In this paper, the upper bound of data rate in 802.11p is set as $R_d = 54$ Mbps, which is an ideal value and not contained in the real modulation and coding scheme (MCS). Thus for comparison, we fix the data rate as $R_d = 24$ Mbps and optimize the λ and W with the proposed scheme. The contention window size is $W = 15$ in the test-bed used parameters, which means the packet would back-off $E(W) = 7.5$ slots on average when they get an idle channel. So in each idle slot, the packet transmission probability would be $p = 1/E(W) = 0.1333$, and the same p is set for the slotted-p-persistent. As for the retransmission strategy, the maximum retransmission times is set as $r_{max} = 3$ [25]. All of these three experiments are performed 7 times with different vehicle locations which follow the same NHPP distribution. And the simulation time is 20 seconds in each experiment.

The results in Fig. 11 show that our solution performs better than the protocols mentioned above in both APP-level reliability and delay. The dashed lines are the results from theoretical analysis and the soiled lines are from simulations. The blue dashed line shows the optimization results of the fixed data rate $R_d = 24$ Mbps (such as 64-QAM), both of the APP-level have a minor reduction compared with the proposed solution, because the data rate could not set as an ideal value. As an improvement solution of CSMA/CA, retransmission strategy could improve the VANETs performance compared with the slotted-p(or 1)-persistent, because of the packets would be retransmitted from the transmitter if the receiver announced a collision. At the same time, with the density of

vehicle increase, the performance of retransmission strategy has a significant decrease, because of the duplicate packets. So it can not perform as well as the proposed solution. Our solution is an optimization scheme based on 802.11p, it is reasonable to infer that other solutions could be improved if the proposed optimization scheme was applied.

5.7. Experiment summary

In this section, several experiments are given in an logical order, and a couple of valuable findings could be derived from the results.

(1) It is feasible to assume that the positions of the vehicles at a signalized intersection follows NHPP in general, which has been validated by SUMO and the K-S test.
(2) The cross-validation between the proposed analytical model and the NS2 simulation shows that the analytical model can be used to evaluate the reliability and performance of VANETs.
(3) We can apply the analytical model to the actual system by combining the measurement of BSMs with the analytical model. In our experiment, we replaced the BSMs collected in the real environment with the locations of the virtual vehicles tracked in NS2.
(4) The VANET performance could not always meet the requirements of the safety applications by only adjusting a signal parameter. In both low and heavy density, the multi-parameter adaptive optimization approach could improve the awareness probability and lower the APP-level delay while maximizing the transmission capacity. The multi-objective multi-parameter adaptive optimization is also verified to be a better solution for ensuring the communication capability of VANETs compared to retransmission and other MAC technologies, i.e. slotted-p(or 1)-persistent.

6. Conclusion

We focus on the reliability and performance analysis and optimization of the BSMs broadcast in IEEE 802.11p based VANETs at the signalized rural intersections. The location of vehicles around the traffic light controlled intersection is simulated by SUMO and validated by the K-S test that it following the NHPP. An analytical model considering the NHPP vehicle locations at the intersection is proposed to evaluate the MAC and APP-level reliabilities. The cross validations with NS2 simulation show the proposed model could characterize the VANET well at the signalized intersection. The number of vehicle related parameters derived from the NS2 simulations are injected into the analytical model directly to imitate its use in actual scenarios, and the results show the execution time has been reduced significantly while the accuracy maintained, that means when applying the proposed model into the real system, the reliability and performance of the VANETs could be calculated in nearly real-time.

In a constantly changing VANET environment, the experiments demonstrate when the communication parameters are fixed, the awareness probability (P_A) and the APP-level delay (D_A) may not always meet the requirements of a specific safety-related application (e.g. CCW). To maximize the QoS constraint transmission capacity (TC), multi-objective single parameter optimization is processed to adjust the packet generation rate (λ) singly, but the results show in the case of high vehicle density, this method will fail due to the heavy traffic ($\beta_{av} = 400$ vehicles/km). Then multiple parameters including λ, contention window W, and data rate R_d are adjusted through a multi-objective multi-parameter adaptive optimization. The experiments show in both low and heavy density, the multi-parameter adaptive optimization approach could improve the P_A and D_A significantly by the optimized parameters while maximizing the TC. And in the optimization, the data rate is adjusted within an ideal upper bound (54 Mbps) or an actual upper bound (24 Mbps in 64-QAM). Out of satisfied combinations of optimized parameters, we consider and select the two combinations of $\lambda = 40$ Hz, $W = 222$, $R_d = 24$ Mbps, and $\lambda = 40$ Hz, $W = 15$, $R_d = 54$ Mbps. The results show that the optimized parameters could meet the stringent APP-level QoS requirements of the safety-related applications, although the P_A and D_A have a slight degradation when the upper bound of R_d is set as 24 Mbps. Comparing with the slotted-p(or 1)-persistent protocol and retransmission strategy, the proposed solution can maximize the TC and getting higher reliability and performance at the same time, and the proposed solution could have more stable APP-level performance than other protocols and strategies.

At the same time, there are also limitation of the proposed model. In the real system, the vehicles would analyze the BSMs and calculate and broadcast the optimized communication parameters periodically according to the environment. If the parameters were reset with a high frequency, the VANET may have a high load and be unstable, but if it has a low update ratio, the optimized parameters may be out of date. So, to make the proposed solution more practical, it is important to figure out what is the best frequency to broadcast and reset the parameters in the future works.

Declaration of Competing Interest

The authors declare that they have no known competing financial interests or personal relationships that could have appeared to influence the work reported in this paper.

Acknowledgment

We would like to thank anonymous reviewers for their invaluable comments and suggestions on improving this work. This work is supported by National Natural Science Foundation of China (NSFC) (grant No. 61572150), and the Fundamental Research Funds for the Central Universities of DUT (No. DUT17RC(3)097).

References

[1] I.W. Group, et al., Ieee standard for information technology–telecommunications and information exchange between systems–local and metropolitan area networks–specific requirements–part 11: Wireless lan medium access control (mac) and physical layer (phy) specifications amendment 6: Wireless access in vehicular environments, IEEE Std. 802 (11) (2010).
[2] E. E. ETSI, 302 665 v1. 1.1: Intelligent transport systems (its), communications architecture, 2010, European Standard (Telecommunications Series)(September 2010).
[3] R. Resendes, Vehicle-to-vehicle and safety pilot, in: Proceedings of US Department of Transportation Safety Workshop, 2010.
[4] A.E. Gómez, S. Glaser, Y. Alayli, A.d.M. Neto, D.F. Wolf, Cooperative collision warning for driving assistance, in: 2016 IEEE 19th International Conference on Intelligent Transportation Systems (ITSC), IEEE, 2016, pp. 990–997.
[5] W. Li, X. Ma, J. Wu, K.S. Trivedi, X.-L. Huang, Q. Liu, Analytical model and performance evaluation of long-term evolution for vehicle safety services, IEEE Trans. Veh. Technol. 66 (3) (2016) 1926–1939.
[6] P. Shen, H. Zou, X. Zhang, Y. Li, Y. Fang, P. Shen, H. Zou, X. Zhang, Y. Li, Y. Fang, Platoon of autonomous vehicles with rear-end collision avoidance through time-optimal path-constrained trajectory planning, in: 2017 11th International Workshop on Robot Motion & Control, IEEE, 2017, pp. 232–237.
[7] X. Yin, Performance and reliability evaluation for dsrc vehicular safety communication, 2013 Ph.D. thesis. Ph.D. thesis, Duke University
[8] X. Ma, X. Yin, K.S. Trivedi, On the reliability of safety applications in vanets, Int. J. Performab. Eng. 8 (2) (2012) 115–130.
[9] P. Papadimitratos, A.L. Fortelle, K. Evenssen, R. Brignolo, S. Cosenza, Vehicular communication systems: Enabling technologies, applications, and future outlook on intelligent transportation, IEEE Commun. Mag. 47 (11) (2009) 84–95.
[10] N. An, T. Gaugel, H. Hartenstein, Vanet: Is 95% probability of packet reception safe? in: 2011 11th International Conference on ITS Telecommunications, IEEE, 2011, pp. 113–119.
[11] X. Yin, X. Ma, K.S. Trivedi, Performance evaluation for dsrc vehicular safety communication: a semi-markov process approach, in: International Conference on Communication Theory, Reliability, and Quality of Service, Citeseer, 2011.

[12] S.E. Carpenter, K. Harfoush, Saferelay: Improving safety in the time-constrained vanet with geoaddresing relay, in: 2017 IEEE International Conference on Vehicular Electronics and Safety (ICVES), IEEE, 2017, pp. 44–50.
[13] J. Zhao, Z. Wu, Y. Wang, X. Ma, Adaptive optimization of qos constraint transmission capacity of vanet, Veh. Commun. (2019).
[14] W. Li, W. Song, Q. Lu, C. Yue, Reliable congestion control mechanism for safety applications in urban vanets, Ad Hoc Netw. 98 (2020) 102033.
[15] S.E. Carpenter, M.L. Sichitiu, Bur-gen: A bursty packet generator for vehicular communication channels, IEEE Trans. Veh. Technol. 67 (11) (2018) 10232–10242.
[16] S. Kühlmorgen, A. González, A. Festag, G. Fettweis, Improving communication-based intersection safety by cooperative relaying with joint decoding, in: 2017 IEEE Intelligent Vehicles Symposium (IV), IEEE, 2017, pp. 679–684.
[17] N. Haouari, S. Moussaoui, S.M. Senouci, Application reliability analysis of density-aware congestion control in vanets, in: 2018 IEEE International Conference on Communications (ICC), IEEE, 2018, pp. 1–6.
[18] S.P. Weber, X. Yang, J.G. Andrews, G. De Veciana, Transmission capacity of wireless ad hoc networks with outage constraints, IEEE Trans. Inf. Theory 51 (12) (2005) 4091–4102.
[19] A.M. Hunter, J.G. Andrews, S. Weber, Transmission capacity of ad hoc networks with spatial diversity, IEEE Trans. Wirel. Commun. 7 (12) (2008) 5058–5071.
[20] S. Weber, J.G. Andrews, N. Jindal, An overview of the transmission capacity of wireless networks, IEEE Trans. Commun. 58 (12) (2010) 3593–3604.
[21] V. Savic, E.M. Schiller, M. Papatriantafilou, Distributed algorithm for collision avoidance at road intersections in the presence of communication failures, in: 2017 IEEE Intelligent Vehicles Symposium (IV), 2017, pp. 1005–1012.
[22] P.A. Lopez, M. Behrisch, L. Bieker-Walz, J. Erdmann, Y.-P. Flötteröd, R. Hilbrich, L. Lücken, J. Rummel, P. Wagner, E. WieBner, Microscopic traffic simulation using sumo, in: 2018 21st International Conference on Intelligent Transportation Systems (ITSC), IEEE, 2018, pp. 2575–2582.
[23] J. Kennedy, Bare bones particle swarms, in: Proceedings of the 2003 IEEE Swarm Intelligence Symposium. SIS'03 (Cat. No. 03EX706), IEEE, 2003, pp. 80–87.
[24] D. Jiang, V. Taliwal, A. Meier, W. Holfelder, R. Herrtwich, Design of 5.9 ghz dsrc-based vehicular safety communication, IEEE Wirel. Commun. 13 (5) (2006) 36–43.
[25] M.I. Hassan, H.L. Vu, T. Sakurai, Performance analysis of the ieee 802.11 mac protocol for dsrc safety applications, IEEE Trans. Veh. Technol. 60 (8) (2011) 3882–3896.
[26] M.I. Hassan, H.L. Vu, T. Sakurai, Performance analysis of the ieee 802.11 mac protocol for dsrc with and without retransmissions, in: 2010 IEEE International Symposium on "A World of Wireless, Mobile and Multimedia Networks" (WoWMoM), 2010, pp. 1–8.
[27] H.P. Luong, M. Panda, H.L. Vu, Q.B. Vo, Analysis of multi-hop probabilistic forwarding for vehicular safety applications on highways, IEEE Trans. Mobile Comput. 16 (4) (2017) 918–933.
[28] L. Kleinrock, F. Tobagi, Packet switching in radio channels: Part i-carrier sense multiple-access modes and their throughput-delay characteristics, IEEE Trans. Commun. 23 (12) (1975) 1400–1416.
[29] the network simulator ns-2, 2008, https://www.isi.edu/nsnam/ns/.
[30] Q. Chen, F. Schmidt-Eisenlohr, D. Jiang, M. Torrent-Moreno, L. Delgrossi, H. Hartenstein, Overhaul of ieee 802.11 modeling and simulation in ns-2, in: Proceedings of the 10th ACM Symposium on Modeling, Analysis, and Simulation of Wireless and Mobile Systems, MSWiM '07, ACM, New York, NY, USA, 2007, pp. 159–168, doi:10.1145/1298126.1298155.
[31] Y. Yao, L. Rao, X. Liu, Performance and reliability analysis of ieee 802.11p safety communication in a highway environment, IEEE Trans. Veh. Technol. 62 (9) (2013) 4198–4212.
[32] X. Ma, M. Wilson, X. Yin, K.S. Trivedi, Performance of vanet safety message broadcast at rural intersections, in: 2013 9th International Wireless Communications and Mobile Computing Conference (IWCMC), IEEE, 2013, pp. 1617–1622.
[33] M. Ni, J. Pan, L. Cai, J. Yu, H. Wu, Z. Zhong, Interference-based capacity analysis for vehicular ad hoc networks, IEEE Commun. Lett. 19 (4) (2015) 621–624.
[34] X. Ma, G. Butron, K. Trivedi, Modeling of vanet for bsm safety messaging at intersections with non-homogeneous node distribution, International Workshop on Communication Technologies for Vehicles, 2016.
[35] V. Nguyen, T.Z. Oo, N.H. Tran, C.S. Hong, An efficient and fast broadcast frame adjustment algorithm in vanet, IEEE Commun. Lett. 21 (7) (2016) 1589–1592.
[36] X. Ma, H. Lu, J. Zhao, Y. Wang, J. Li, M. Ni, Comments on "interference-based capacity analysis of vehicular ad hoc networks", IEEE Commun. Lett. 21 (10) (2017) 2322–2325.
[37] H.P. Luong, M. Panda, H.L. Vu, B.Q. Vo, Beacon rate optimization for vehicular safety applications in highway scenarios, IEEE Trans. Veh. Technol. 67 (1) (2017) 524–536.
[38] A. Patel, P. Kaushik, Improve qos of ieee 802.11 p using average connected coverage and adaptive transmission power scheme for vanet applications, Wirel. Pers. Commun. 95 (4) (2017) 3829–3855.
[39] M. Noor-A-Rahim, G.M.N. Ali, H. Nguyen, Y.L. Guan, Performance analysis of ieee 802.11 p safety message broadcast with and without relaying at road intersection, IEEE Access 6 (2018) 23786–23799.
[40] T. Kimura, H. Saito, Theoretical performance analysis of vehicular broadcast communications at intersection and their optimization, in: 2019 31st International Teletraffic Congress (ITC 31), IEEE, 2019, pp. 37–45.
[41] J. Zhao, Z. Li, Y. Wang, Z. Wu, X. Ma, Y. Zhao, An analytical framework for reliability evaluation of d-dimensional ieee 802.11 broadcast wireless networks, in: Wireless Networks, 2020, pp. 1–22.
[42] H. Cheng, Y. Yamao, Reliable inter-vehicle broadcast communication with sectorized roadside relay station, in: 2013 IEEE 77th Vehicular Technology Conference (VTC Spring), 2013, pp. 1–5.
[43] F. Bai, H. Krishnan, T. Elbatt, G. Holland, Towards characterising and classifying communication-based automotive applications from a wireless networking perspective, Int. J. Veh. Auton. Syst. 10 (3) (2012) 165–197.
[44] H. Lu, C. Poellabauer, Analysis of application-specific broadcast reliability for vehicle safety communications, in: Proceedings of the Eighth ACM International Workshop on Vehicular Inter-Networking, ACM, 2011, pp. 67–72.
[45] the network simulator ns-3, 2008, https://www.nsnam.org/.
[46] N. Lu, X.S. Shen, Capacity Analysis of Vehicular Communication Networks, Springer, 2014.
[47] K. Alvehag, L. Soder, A reliability model for distribution systems incorporating seasonal variations in severe weather, IEEE Trans. Power Del. 26 (2) (2011) 910–919.
[48] M. Killat, H. Hartenstein, An empirical model for probability of packet reception in vehicular ad hoc networks, EURASIP J. Wirel. Commun. Netw. 2009 (2009) 4.
[49] R. Hajlaoui, H. Guyennet, T. Moulahi, A survey on heuristic-based routing methods in vehicular ad-hoc network: Technical challenges and future trends, IEEE Sensor. J. 16 (17) (2016) 6782–6792.
[50] J. Kennedy, R. Eberhart, Particle swarm optimization, in: IEEE International Conference on Neural Networks, 1995. Proceedings, 2002, pp. 1942–1948. Vol.4
[51] M. Karamouz, S. Nazif, M. Falahi, Hydrology and hydroclimatology: principles and applications, CRC Press, 2012.
[52] R.C. Poonia, R. Dadhich, X.Z. Gao, Simulation-based efficient analysis of radio propagation model using on-demand routing protocols in the Indian automotive networks, Int. J. Auton. Adapt. Commun. Syst. 11 (1) (2018) 68–82.
[53] X. Ma, X. Chen, Delay and broadcast reception rates of highway safety applications in vehicular ad hoc networks, in: 2007 Mobile Networking for Vehicular Environments, IEEE, 2007, pp. 85–90.
[54] X. Yin, X. Ma, K.S. Trivedi, Channel fading impact on multi-hop dsrc safety communication, in: Proceedings of the 16th ACM International Conference on Modeling, Analysis & Simulation of Wireless and Mobile Systems, ACM, 2013, pp. 443–446.
[55] C.V.S.C. Consortium, et al., Vehicle safety communications project: Task 3 final report: identify intelligent vehicle safety applications enabled by dsrc, National Highway Traffic Safety Administration, US Department of Transportation, Washington DC, 2005.
[56] B.-J. Chang, J.M. Chiou, Cloud computing-based analyses to predict vehicle driving shockwave for active safe driving in intelligent transportation system, IEEE Transactions on Intelligent Transportation Systems, 2019.
[57] T. Zinchenko, H. Tchouankem, L. Wolf, Reliability analysis of vehicle-to-vehicle applications based on real world measurements, in: Proceeding of the Tenth ACM International Workshop on Vehicular Inter-Networking, Systems, and Applications, 2013, pp. 11–20.
[58] S.E. Shladover, Effects of traffic density on communication requirements for cooperative intersection collision avoidance systems (cicas), 2005,
[59] X. Ma, G. Kanelopoulos, K.S. Trivedi, Application-level scheme to enhance VANET event-driven multi-hop safety-related services, in: 2017 International Conference on Computing, Networking and Communications (ICNC), IEEE, 2017, pp. 860–864.
[60] B. Bilgin, V. Gungor, Performance comparison of ieee 802.11 p and ieee 802.11 b for vehicle-to-vehicle communications in highway, rural, and urban areas, Int. J. Veh. Technol. 2013 (2013).

Yanbin Wang received the PhD degree from the Industrial Engineering Department, Harbin Institute of Technology of China, in 2007. He is currently an associate professor in the department of Industrial Engineering, School of Mechatronics Engineering, Harbin Institute of Technology of China. His research interests include quality management, scheduling, optimization, physical layer and MAC layer of vehicular ad hoc wireless networks.

Zhuofei Wu received the B.Eng. and M.Eng. degrees in College of Ship Building Engineering at Harbin Engineering University, China. Currently, He is working toward the PhD degree in Computer Science and Technology at Harbin Engineering University, China. His research interests include reliability evaluation and performance optimization of Vehicle Ad-Hoc Network.

Jing Zhao received Ph.D. (2006) degree in computer science and Technology in Harbin institute of Technology of China. In 2010 she was with Department of Electrical and Computer Engineering at Duke University, Durham, NC, working as a Postdoc under supervision of Dr. Kishor Trivedi. She is currently a Professor in the School of Software Technology, Dalian University of Technology of China. Her research interests include reliability engineering, software aging theory, vehicle ad-hoc network and dependability modeling.

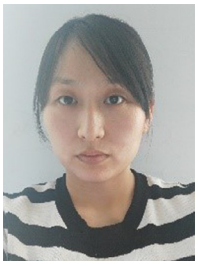

Zhijuan Li received the M.S. degree at the School of Computer Science and Technology, Harbin Engineering University, Harbin, China, in 2013. From 2013 to 2016, she was a software engineer with Harbin Yuguang Virtual Network Technology Co., Ltd, China. She is currently working toward the Ph.D. degree with the School of Computer Science and Technology, Harbin Engineering University. Her research interests include vehicular ad hoc network and fog computing.

Xiaomin Ma (M'03-SM'08) received the B.E. degree from Anhui University, Hefei, China; the M.E. degree in electrical engineering from the Beijing University of Aerospace and Aeronautics, Beijing, China; and the Ph.D. degree in information engineering from the Beijing University of Posts and Telecommunications, Beijing, China, in 1999. From 2000 to 2002, he was a Postdoctoral Fellow with the Department of Electrical and Computer Engineering, Duke University, Durham, NC, USA. He is currently a Professor with the Department of Engineering, Oral Roberts University, Tulsa, OK, USA. His research interests include stochastic modeling and analysis of computer and communication systems; physical layer and medium-access layer of vehicular ad hoc wireless networks; computational intelligence and its applications to coding, signal processing, and control; and quality of service and call admission control protocols in wireless networks.